Journal of Applied Polymer Science

On the Non-Newtonian Viscous Behavior of Polymer Melts in Terms of Temperature and Pressure-Dependent Hole Fraction

Fatma Sahin Dinc,[1] Tomas Sedlacek,[2] Cumali Tav,[1] Ugur Yahsi[1]

[1]Physics Department, Faculty of Arts and Sciences, Marmara University, Goztepe Campus, 34722 Kadikoy, Istanbul, Turkey
[2]Centre of Polymer Systems, University Institute, Tomas Bata University in Zlin, Zlin, Czech Republic
Correspondence to: F. S. Dinc (E-mail: s_fatm@hotmail.com)

ABSTRACT: A new theoretical non-Newtonian viscosity model is developed by taking the fractional series expansion of Eyring's shearing strain rate. A broad range of experimental rheological data of various polymer melts including polyethylenes, polypropylene, polystyrene, poly (methyl methacrylate), and polycarbonate are fitted well using the proposed model. From the model; zero shear, constant shear-stress and constant shear-rate viscosities are derived as a linear function of viscosity related quantity, Y_h, called "thermo-occupancy function" and their coefficients are discussed in detail. The thermo-occupancy function is expressed in terms of temperature and structural vacancies such as hole fraction computed from the Simha-Somcynsky Hole Theory (SS). In addition, the derivative of the logarithm of viscosities with respect to the hole fraction, named as viscoholibility, is observed decreases with the increasing hole fraction. © 2014 Wiley Periodicals, Inc. J. Appl. Polym. Sci. **2014**, *131*, 40540.

KEYWORDS: polycarbonates; polyolefins; polystyrene; rheology; theory and modeling

Received 10 December 2013; accepted 3 February 2014
DOI: 10.1002/app.40540

INTRODUCTION

For polymeric liquids, viscosity in terms of shear-rate, described by the viscosity curves, is classified as Newtonian viscosity (linear viscosity), η_0, and non-Newtonian viscosity. The non-Newtonian viscosity plays an important role in describing their characteristic properties. Several practical and theoretical non-Newtonian viscosity models exist in the literature. Two well-known models, Cross and Carreau[1,2] are widely used in correlating viscosity with shear-rate. Hieber and Chiang[1] fitted their shear viscosity data in terms of generalized Cross/Carreau model for the shear-rate dependence. They showed that the Cross model gives a better fit than the Carreau model. Kadijk and Van Den Brule[2] described the viscosity at high shear-rates for PP, PS and ABS with the use of the two-parameter generalized Cross/Carreau equation. While they fitted the data excellently for PS and ABS, the fitting is reasonable for PP. Sedlacek et al.[3] used another multi-parameter model, Carreau-Yasuda equation,[3,4] involving exponential relation of pressure and temperature, to fit their non-Newtonian viscosity data. As an extension to these models, in this paper, we propose a theoretical model for non-Newtonian viscosity by taking the fractional Taylor expansion of the exponential product of Eyring's rate of shearing strain.[5–8] Our proposed model works successfully on both temperature and pressure dependent zero shear viscosities and critical shear-stress parameters with a single fitting parameter.

Another interesting approach is free volume dependency of viscosity that has been a promising asset to describe the flow behavior of polymer melts. In this regard, some correlations between free volume and viscosity have been presented by several researchers. One of these is given by well-known Doolittle's viscosity-free volume relation.[3,9,10] Moreover, as a modification of Doolittle's free volume model, Utracki[11–13] related zero shear viscosity inversely with hole fraction computed from the SS theory. However, extending it for more complicated structures, Yahsi[5,6,14] proposed a new theoretical derivation for zero shear viscosity as a function of temperature and pressure dependent hole fraction, $h(T,P)$, computed from an equilibrium property of the SS theory. He applied it successfully for some branched hydrocarbons, their mixtures and polymers.[6,15,16]

Sorrentino and Pantani[17] found a linear relationship between the logarithm of zero shear viscosity and inverse of free volume by using Doolittle's equation while Sedlacek et al.[3] modified Utracki's form of the hole fraction model to linearize zero shear and constant shear-stress viscosities data. In this article, we extend zero shear and constant shear-stress work mentioned above to constant shear-rate viscosities as well. We also define the derivative of the logarithm of viscosity at constant shear-stress and constant shear-rate and observe them to decrease as the whole fraction increases.

Hence, a non-Newtonian viscosity model that is a function of the zero shear viscosity, η_0, and the critical stress parameter, τ,

is established. The experimental rheological data at a wide range of *T-P* values are fitted through this proposed model and 2–3 folds less deviation is obtained than the Cross Model at high pressures. Furthermore, by using the experimental *PVT* data some relationships among *PVTh* values are stated both with the SS Theory and with the obtained various Tait like equations. The linear dependency of our derived viscosity quantities (zero shear viscosity, constant stress viscosity, and constant shear-rate viscosity) with hole fraction (h) and temperature (T) dependent thermo-occupancy function (Y_h) are also presented. It is found that the derivative of the logarithms of the viscosities with respect to h (viscoholibility) decreases with h increases.

THEORIES

The SS-EOS Theory

Simha and Somcynsky (SS)[18] developed an equation of state (EOS) based on the lattice-hole model providing $\tilde{P}=\tilde{P}\left(\tilde{V},\tilde{T},h\left(\tilde{V},\tilde{T}\right)\right)$ derived from the configurational Helmholtz energy:

$$\tilde{P}\tilde{V}/\tilde{T}=(1-Q)^{-1}+(2y/\tilde{T})(y\tilde{V})^{-2}[1.011(y\tilde{V})^{-2}-1.2045] \quad (1)$$

which is formulated in terms of volume, temperature, and pressure in scaled forms, viz. $\tilde{V}=V/V^*$, $\tilde{T}=T/T^*$ and $\tilde{P}=P/P^*$. For an s-mer, V^* is defined by $N_A\upsilon^*/m_0$, where N_A is the Avogadro's number, m_0 is the molar mass of a segment, and characteristic molar volume υ^* of a segment given by the segmental location r^* of the potential minimum. T^* equals to $q_z\varepsilon^*/ck$ as a balance between attraction and thermal energy contributed by the external degrees of freedom ($3c$) where attractive interaction parameter ε^* of a segment corresponds to the potential minimum. Accordingly, P^* is defined by the ratio between chain attraction energy $q_z\varepsilon^*$ and chain hard core volume $s\upsilon^*$, where q_z is the number of the first neighbor intermolecular pairs of the s-mer (chain length of a polymer), viz., $s(z-2)+2$ with the coordination number z.

SS-EOS is defined in terms of occupied site fraction, y, to be computable by minimization of Helmholtz energy of an ensemble, $\partial F/\partial y|_{\tilde{V},\tilde{T},c/s}=0$:

$$\begin{aligned}(s/3c)[(s-1)/s+y^{-1}\ln(1-y)]&=(Q-1/3)/(1-Q)\\&+(y/6\tilde{T})(y\tilde{V})^{-2}\left[2.409-3.033(y\tilde{V})^{-2}\right]\end{aligned} \quad (2)$$

where $Q=2^{-1/6}y(y\tilde{V})^{-1/3}$. The SS-EOS has been applied to low and high-molecular-weight systems to describe their thermodynamical properties and extended to interpret the non-equilibrium properties, viz. viscoelasticity, physical aging etc. The hole fraction has been also utilized to express a variety of equilibrium and kinetic process such as viscosity,[2,3,12,13,19] ionic conductivity[20] etc.

The non-Newtonian Viscosity Model

The Eyring's rate of shearing strain was defined by the use of the rate of a relative displacement of adjacent layers with forward and backward terms per unit length between two successive layers denoted by λ_1 as

$$\dot{\gamma}=\sum_i\left(\frac{\lambda\cos\theta_i}{\lambda_1}\right)k_i\exp(\xi_i\sigma/kT)(1-\exp(-2\xi_i\sigma/kT)) \quad (3)$$

where $\xi_i=\lambda_2\lambda_3\lambda\cos\theta_i/2$ and the term, $\xi_i\sigma$, gives the work done by the shear-stress, σ, that is applied on the surface area $\lambda_2\lambda_3$ occupied by a segment, displaced by $\lambda\cos\theta_i/2$ to the top of a barrier (the half way to the next minimum potential) for the ith segment. The jumping frequency, k_i, is assumed to be similar on the average for all available positions for each molecular segment and given by[5–8,21]

$$k'=\kappa\frac{kT}{h_p}\exp\left(\frac{-E_a}{kT}\right) \quad (4)$$

where h_p is the Planck's constant, k is the Boltzman's constant, κ is the transmission coefficient, and E_a is the activation energy. The activation energy, given by the following expression

$$E_a=\frac{1}{2}\frac{1-h}{h}a'q_z\Phi \quad (5)$$

is the necessary energy for a molecular segment to jump into a hole in which a' is proportionality constant, q_z is the number of interchain nearest neighboring pairs, Φ is the interaction potential energy between a pair of segments.

The series expansion of the last product in eq. (3) can be approximated by keeping the non-vanishing term: $2\xi_i\sigma/kT$. On the other hand, the first exponential product, $\exp(\xi_i\sigma/kT)$, in the same equation needs a special handling in such a way that its fractional Taylor expansion can be expanded about η_0 (or $\dot{\gamma}\to 0$)[22]

$$e^{\xi_i\sigma/kT}|_{\eta_0}=\sum_{n=0}^{\infty}\frac{(\xi_i\eta_0\dot{\gamma}/kT)^{nq}}{\Gamma(nq+1)}. \quad (6)$$

where q is the order of the fractional derivative of the exponential function employed in the expansion given below[23]

$$\frac{d^q e^{ax}}{dx^q}=a^q e^{ax}. \quad (7)$$

Keeping the terms up to $2q$ powers of shear-rate in the expansion of eq. (6) and substituting eqs. (3–7) in the viscosity equation, defined as the ratio of shear-stress to shear-rate, the following expression is obtained

$$\eta=\frac{\eta_0}{1+\frac{\theta_1}{\Gamma(q+1)}\left(\frac{\eta_0\dot{\gamma}}{\tau}\right)^q+\frac{\theta_2}{\Gamma(2q+1)}\left(\frac{\eta_0\dot{\gamma}}{\tau}\right)^{2q}} \quad (8)$$

where $\Gamma(q)$ is a gamma function, $\theta_n=\frac{2}{\pi}\sum_i\cos^{nq+2}\theta_i$, $(n=1,2)$, and $\tau=4RT/\sqrt{6}\upsilon$. Here the zero-shear viscosity[16] defined as the zeroth order approximation of eq. (8) is $\eta_0=\eta^* e^{E_a/kT}$. Substituting eq. (5) in this expression and taking the logarithm of both sides we obtain

$$\ln\eta_0=\ln\eta^*+\alpha Y_h,\ Y_h=\frac{1-h}{h}\frac{1}{T} \quad (9)$$

in which the parameters η^* and α are given

$$\eta^*=\frac{\sqrt{2}N_A h_p}{\pi\kappa\upsilon}\ \text{and}\ \alpha=a'\frac{q_z\Phi}{2k} \quad (10)$$

where υ is the molar volume of a segment of a polymer. Here υ and Φ quantities are slowly varying functions comparing with

viscosity so that they are kept in the coefficients of eq. (9).[5,6,15] Here the quantity, Y_h, is a ratio of a number of occupied sites to unoccupied sites (holes) divided by the absolute temperature; it can be interpreted as the number of occupied sites for each empty site per unit temperature. Thus, Y_h contributes to the calculation of viscosity in two folds: First, it depends on the structural occupancy; second, it is inversely related to temperature which is also correlated with vibrational energy. Because of such importance of this contribution to our calculations, we would name Y_h as "thermo-occupancy function."

Neglecting $2q$ power term in eq. (8) reduces to an equation similar to the formula given by the Cross model as

$$\eta = \frac{\eta_0}{1+\frac{\theta_1}{\Gamma(q+1)}\left(\frac{\eta_0\dot{\gamma}}{\tau}\right)^q}. \tag{11}$$

As having a great essence of viscosity-hole fraction behavior, the derivative of eq. (9) with respect to h at constant T is defined and coined a name "viscoholibility" (as a combination of viscosity and hole fraction) is given as follows:[16]

$$\left.\frac{\partial \ln \eta_0}{\partial h}\right|_T = -\frac{\alpha}{h^2 T} \tag{12}$$

In a similar manner, the derivative of logarithmic viscosity with respect to h at constant shear-stress can be derived using eqs. (3–5) with an assumption of Φ to be constant:

$$\left.\frac{\partial \ln \eta}{\partial h}\right|_{\sigma,T} = -\left.\frac{\partial \ln \dot{\gamma}}{\partial h}\right|_{\sigma,T} \cong -\frac{\alpha}{h^2 T} \tag{13}$$

Similar to eqs. (12) and (13) the derivative of logarithmic viscosity at constant shear-rate can be predicted by

$$\left.\frac{\partial \ln \eta}{\partial h}\right|_{\dot{\gamma},T} = -\frac{\alpha}{h^2 T} \tag{14}$$

From eqs. (13) and (14), the viscosity at constant shear-stress and constant shear-rate can be written similar to eq. (9):

$$\ln \eta|_\sigma = \ln \eta^* + \alpha Y_h \text{ and } \ln \eta|_{\dot{\gamma}} = \ln \eta^* + \alpha Y_h. \tag{15}$$

where η^* and α in eqs. (13–15) change with constant shear-stress and constant shear-rate. Here the expressions in eqs. (13) and (14) will be called as "viscoholibility at constant shear-stress" and "viscoholibility at constant shear-rate," respectively.

CALCULATIONS

The Scaling Parameters of the SS Theory

We have studied *PVT* behavior of some commercially available polymers such as high-density polyethylene (HDPE), low-density polyethlylene (LDPE), linear low-density polyethylene (LLDPE), polypropylene (PP), polystyrene (PS), poly(methyl methacrylate) (PMMA), polycarbonate (PC). Their experimental *PVT* and viscosity data were reported by Sedlacek et al.[3,24] in the temperature range 70–290°C and the pressure range 15–70 MPa with the increments of 5 MPa.

Using the *PVT* data of these polymers, the scaling parameters P^*, V^*, T^* and the structural flexibility parameter $3c/s$ with $3c = s+3$ have been computed from eqs. (1) and (2).[6,15] The optimized s values correspond to an ideal chain case. The scaling parameters P^*, V^*, T^* are computed by superimposing the experimental *PVT* data on the theoretical $\tilde{P}\tilde{V}\tilde{T}$ surface. To do this, first, the parameter c is assumed as an adjustable parameter, and then the set of the experimental data is projected on the theory to get an equation in terms of V^* and T^* including P^*. Second, expanding each up to the first power in V^* and T^*, N equations are obtained from the N *PVT* data and solved for two unknowns V^* and T^* using the Pseudo Inverse Matrix Technique. The best c values with the scaling parameters P^*, V^*, T^* are taken by the least mean percentage error in specific volume defined by

$$\Delta V(\%) = \frac{100}{N}\sum_i \frac{|V_i^{\exp} - V_i^{calc}|}{V_i^{\exp}}. \tag{16}$$

The obtained parameters with the mean and maximum percentage error in specific volume are reported in Table I for the polymers. The mean percentage deviation ranges from 0.028 to 0.077% (on the average: 0.054%) and the maximum percentage error is 0.45% for PS and less for the other polymers. These parameters are ready to be used for the computational hole fraction, then for the viscosity and their derivative models.

To determine the *PVT* behavior of all the samples, the Tait equation,[18,25] a highly accurate approximation to the solution of the coupled eqs. (1) and (2), is available at atmospheric pressure in a scaled isobar as

Table I. Scaling Parameters Computed from eqs. (1) and (2) with Testing Temperature Ranges

Polymer	Temperature range (°C)	$10^3 \times m_0$ (kg)	s	$\langle -\Phi/k \rangle$[a] (K)	$10^3 \times V^*$ ($m^3 kg^{-1}$)	T^* (K)	P^* (MPa)	ΔV%	Max ΔV%
LDPE	70-210	40.25	2037	502.4	1.1718	10494	617.6	0.029	0.12
LLDPE	70-210	40.61	1467	508.9	1.1752	10623	618.1	0.028	0.18
HDPE	90-230	33.27	2877	425.9	1.1834	8900	627.2	0.057	0.37
PMMA	130-270	37.46	2907	461.8	0.8364	9649	854.3	0.066	0.39
PC	120-290	42.73	402	467.8	0.8157	9715	778.3	0.069	0.42
PP	110-250	38.97	4911	432.5	1.1755	9042	547.4	0.054	0.31
PS	140-290	42.36	6657	472.7	0.9560	9881	676.6	0.077	0.45

[a] The values listed for $\langle -\Phi/k \rangle$ differ within ±0.7

$$\ln \tilde{V} = a'_0 + a'_1 \tilde{T}^{3/2} \quad (17)$$

where $a_0' = -0.09504$ and $a_1' = 22.992$ in this work. We propose an approximate scaled volume–temperature relationship in a full range of pressures as

$$\ln \tilde{V} = \frac{1}{a_0 + b_0 \tilde{P}} + \frac{1}{a_1 + b_1 \tilde{P} + c_1 \tilde{P}^2} \tilde{T}^{\frac{3}{2}} \quad (18)$$

where the coefficients are fitted for all the species as: $a_0 = -10.522 \pm 0.011$, $b_0 = -0.576 \pm 0.165$, $a_1 = 0.04349 \pm 0.000019$, $b_1 = 0.1595 \pm 0.0003$, and $c_1 = 0.08209 \pm 0.00332$, using specific volumes calculated by eqs. (1) and (2) for the ranges of temperatures on Table I and 15–70 MPa pressures. Comparing the specific volume computed by eq. (18) with the SS results, we obtained the mean and maximum deviations 0.04% and 0.18%, respectively. Equation (18) includes five fitting parameters, so it provides less deviation than the three-parameter SS Theory.

The hole fraction data determined from SS theory were fitted into the scaling relationship for the *h*-*P*-*T* behavior of polymers in a full range of pressures and temperatures

$$h = \frac{1}{h_0 + h_1 \tilde{P}} + \frac{\tilde{T}}{h_2 + h_3 \tilde{P}} \quad (19)$$

where $h_0 = -8.479 \pm 0.006$, $h_1 = -22.58 \pm 0.10$, $h_2 = 0.1660 \pm 0.0001$, and $h_3 = 0.4682 \pm 0.0008$. The hole fraction, $h(\tilde{T},\tilde{P})$ computed from eq. (19) using all the species shows mean and maximum deviation of 0.10% and 0.48%, respectively, from the SS Theory.

The Shear Viscosity Calculations

The experimental rheological data for the polymers studied were reported by Sedlacek et al.[3,24] for three tested temperatures and six pressures (0.1, 10, 20, 35, 50, and 70 MPa). Now, these sets of data are fitted for each polymer using eqs. (8) and (11) with the double and single non-vanishing term(s) in the denominator, respectively, to obtain the zero shear viscosities, η_0, and the shear-stress parameters, τ, along with the fraction q as a nonlinearity parameter in the power of shear-rate. Our motivation is to obtain η_0 and τ for each temperature and pressure data set while q is a sole parameter for each polymer. To obtain η_0 and τ, we employ nonlinear fit scheme assuming that q is taken as a disposable quantity. The best q value is adjusted with the least mean percentage error in viscosity defined as

$$\Delta\eta(\%) = \frac{100}{N} \sum_i \left| 1 - \frac{\eta_i^{calc}}{\eta_i^{exp}} \right|. \quad (20)$$

At atmospheric pressure the viscosity data are given at low shear-rate (0.1–10 s^{-1}) as well as high shear-rate (up to 8500 s^{-1}), so these data set can be used to obtain η_0 and τ as well as q parameter explained above scheme (PC, PMMA, and PS are considered at high shear-rate). By fixing q, we can obtain all η_0 and τ at different pressures other than the ambient pressure because the viscosity data are available only at high shear-rates (35–8500 s^{-1}). To reduce figure crowding, we demonstrated only HDPE at Figures 1–4. Logarithmic viscosity versus logarithmic shear-rate is plotted at various temperatures at ambient pressure in Figure 1 and for various pressures only at 210°C in Figure 2. Similar plots are obtained for the other polymers

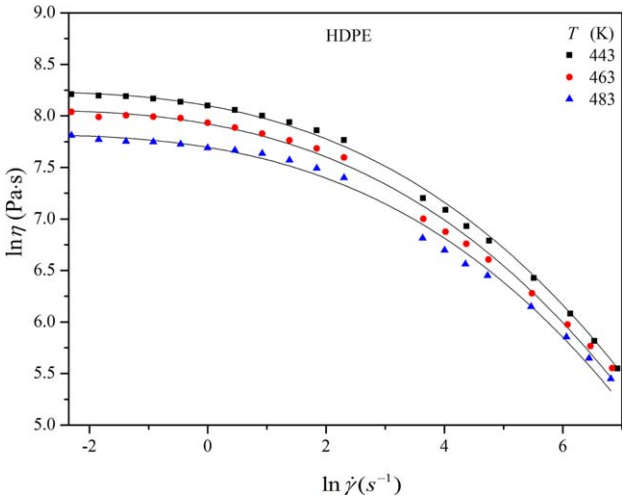

Figure 1. Logarithm of viscosity versus logarithm of shear-rate of HDPE at atmospheric pressure and various temperatures. Solid lines represent data fitting by eq. (8). [Color figure can be viewed in the online issue, which is available at wileyonlinelibrary.com.]

given in Table II. The solid line is drawn by eq. (8) with the best fit parameters. These parameters at ambient pressure are collected in Table II with the mean percentage error in viscosity by eq. (20) and R^2 as the correlation coefficient squared. In a similar manner, the parameters in eq. (11) are also tabulated in parenthesis in Table II at ambient pressure only. For HDPE, the mean percentage errors in viscosity at ambient pressure are 2.85, 4.53, and 5.14% for the temperatures 170, 190, and 210°C, respectively. It drops to about 1% or less at higher pressures; the exact values are 1.14, 0.80, and 0.73 [3.29, 2.43, 2.03 using for eq. (11)] for the respective temperatures, as noticed easily in Figures 1 and 2. The mean percentage errors in viscosity for all the polymers accounted are less than 5.30% at ambient and

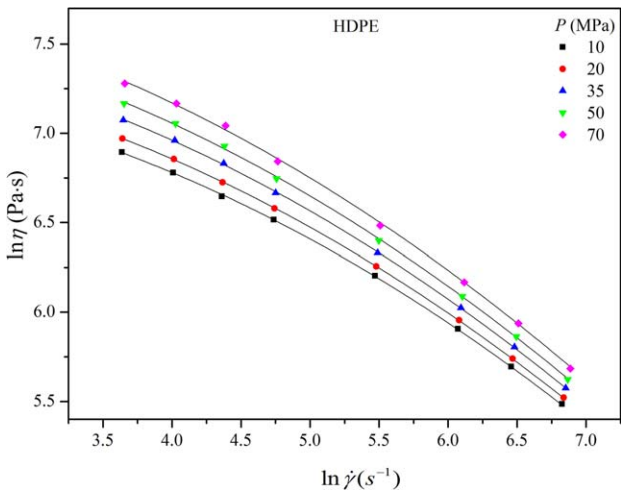

Figure 2. Logarithm of viscosity versus logarithm of shear-rate of HDPE at 210°C and various pressures. Solid lines represent data fitting by eq. (8). [Color figure can be viewed in the online issue, which is available at wileyonlinelibrary.com.]

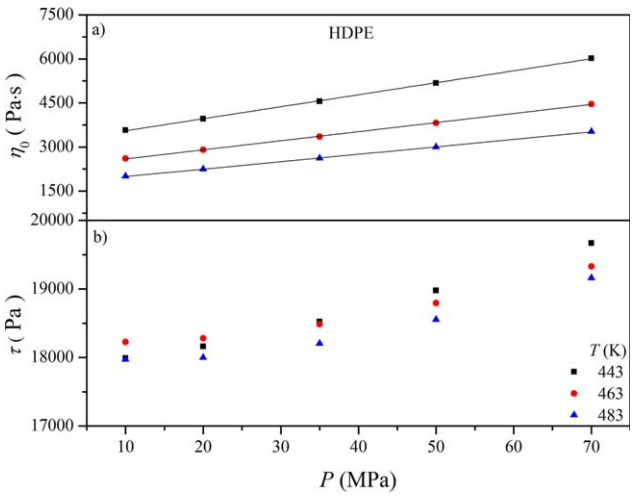

Figure 3. Zero-shear viscosities, η_0, and critical shear-stress parameter, τ, computed by eq. (8), with respect to pressures for HDPE at different temperatures. Solid lines represent linear fitting through the data. [Color figure can be viewed in the online issue, which is available at wileyonlinelibrary.com.]

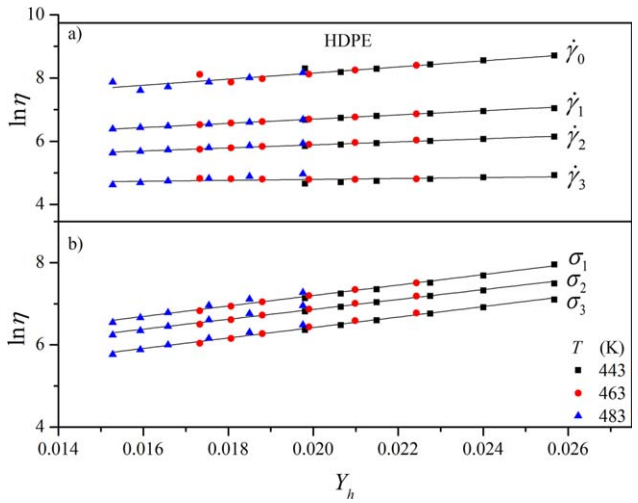

Figure 4. The logarithm of viscosities versus thermo-occupancy function Y_h for HDPE (a) at the zero shear and the constant shear-rates ($\dot{\gamma}_c$ = 148, 665, 2980 s^{-1}), and (b) constant shear-stresses (σ_c = 60, 99, 163 kPa). Solid lines represent linear fitting through each data set by eqs. (9) and (15) with the parameters tabulated in Tables III–V. [Color figure can be viewed in the online issue, which is available at wileyonlinelibrary.com.]

4.40% at higher pressures. However, using eq. (11), the mean percentage errors are less than 3.45% at ambient pressure and 9.89% at higher pressures. Even though the mean percentage error at ambient pressure decreases slightly according to eq. (11) except LLDPE and PS, it increases by a factor of almost two for HDPE, LLDPE and PS and three for PP at higher pressures, hence eq. (11) still reasonably fits the viscosity data. Thus, eq. (8) at high pressure, eq. (11) at ambient pressure work fine. Moreover, in Figure 3, the zero shear-rate viscosity and the shear-stress parameter are plotted as a function of

Table II. Rheological Parameters Computed from eqs. (8) and (11) in Parenthesis in Terms of Three Different Temperatures at Ambient Pressure

Polymer	T(°C)	q	η_0 (Pa s)	τ(Pa)	$\Delta\eta$ (%)	R^2
LDPE	150	0.531 (0.614)	2522.68 (2394.74)	3334.2 (2443.7)	3.49 (1.90)	0.99932 (0.99959)
	170		1424.26 (1362.49)	4170.5 (3020.1)	5.41 (3.15)	0.99794 (0.99893)
	190		837.743 (804.405)	3654.5 (2627.6)	5.60 (3.99)	0.99752 (0.99863)
LLDPE	150	0.540 (0.615)	1216.96 (1190.66)	15870.5 (10490.3)	2.45 (3.31)	0.99907 (0.99934)
	170		785.803 (770.735)	16967.3 (11139.7)	2.85 (3.06)	0.99830 (0.99874)
	190		553.174 (542.731)	14529.5 (9498.1)	3.52 (3.97)	0.99910 (0.99912)
HDPE	170	0.540 (0.625)	3992.81 (3859.32)	15398.7 (10086.8)	2.85 (2.36)	0.99930 (0.99965)
	190		3342.51 (3231.93)	13041.0 (8528.7)	4.53 (3.14)	0.99880 (0.99930)
	210		2620.53 (2536.59)	12148.1 (7935.1)	5.14 (4.28)	0.99835 (0.99893)
PMMA	230	0.537 (0.854)	24751.7 (8045.98)	7293.2 (3828.3)	4.37 (0.86)	0.99991 (0.99992)
	240		9391.97 (3570.63)	7673.7 (3703.6)	1.46 (2.37)	0.99997 (0.99975)
	250		3686.98 (1722.57)	8310.9 (3492.0)	5.70 (1.95)	0.99968 (0.99991)
PC	280	0.532 (0.537)	108.089 (108.355)	91652.8 (84144.8)	1.95 (1.91)	0.99931 (0.99931)
	290		94.432 (94.729)	56898.1 (52057.5)	0.44 (0.41)	0.99997 (0.99998)
	300		84.081 (85.399)	18894.9 (16425.3)	1.94 (2.11)	0.99953 (0.99945)
PP	190	0.557 (0.684)	2082.62 (1947.16)	3845.5 (1988)	4.34 (2.01)	0.99955 (0.99998)
	210		1515.34 (1422.46)	3815.1 (1965.8)	4.42 (2.41)	0.99899 (0.99975)
	230		1076.46 (1014.55)	3522.0 (1804.6)	7.14 (4.45)	0.99646 (0.99838)
PS	190	0.447 (0.759)	26304.64 (7085.02)	955.162 (1654.0)	5.36 (3.27)	0.99949 (0.99967)
	210		5899.28 (1442.18)	1150.8 (2092.6)	1.90 (2.54)	0.99985 (0.99991)
	230		2892.69 (752.878)	1048.2 (1836.1)	0.80 (1.33)	0.99996 (0.99990)

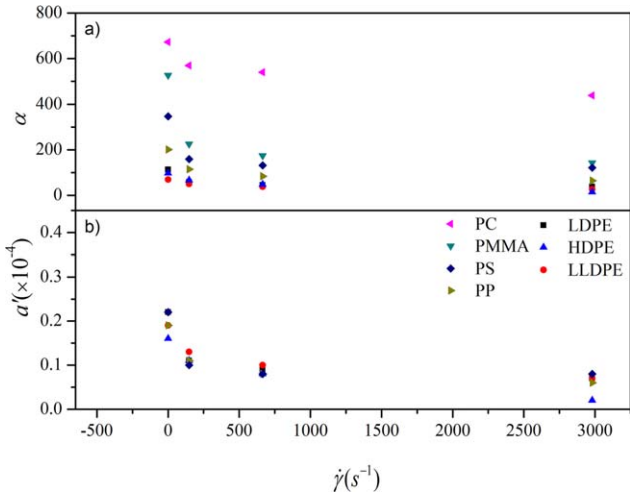

Figure 5. The shear-rate dependency of computed α and a' parameters for the polymers in Table I calculated by eqs. (10) and (15). [Color figure can be viewed in the online issue, which is available at wileyonlinelibrary.com.]

pressure at various temperatures for HDPE. For the zero shear viscosity graph, it is included the best fit line. The zero shear viscosity increases linearly with increasing pressure, but the shear-stress parameter, depending on pressure in terms of T/v, increases but not consistently in temperature. On the other hand, the zero shear viscosity decreases steadily with increasing temperature, but we may not draw an exact temperature dependency on the shear-stress parameter.

Free Volume Relation of Viscosities Under Zero Shear, Constant Shear-Stress, and Constant Shear-Rate

Correlation can be made between hole fraction and viscosities at constant shear-stress and constant shear-rate given in eqs. (13) and (14) obtained from the viscosity data in terms of shear-rate and shear-stress. First, shear viscosity is fitted with respect to shear-stress by a fourth order polynomial equation and then the interpolating η_σ values are calculated at certain constant shear-stresses, σ_c (say, 36, 60, 99 kPa for PP, LLDPE, LDPE; 60, 99, 163 kPa for HDPE; 89 kPa for PS and PC; 163 and 243 kPa for PMMA) at the three tested temperatures and six pressures. Similarly, the constant shear-rate viscosities, $\eta_{\dot{\gamma}}$, are calculated at certain constant shear-rates, $\dot{\gamma}_c$(say 148, 665 and 2980 s^{-1} for all polymers) at the three tested temperatures and various pressures.

The relations for the calculated zero shear given by eq. (9), the constant shear-rate and the constant shear-stress viscosities given by eq. (15) are tested in terms of hole fraction computed from the SS theory discussed above. In Figure 4, the logarithms of zero-shear, constant shear-rate and the constant shear-stress viscosities are plotted with respect to the thermo-occupancy function, Y_h, for HDPE and the solid lines are drawn through the data with the best fit line. A good linearization for three different viscosity schemes for each polymer is obtained for the three tested temperatures and all the given pressures. In the figure for each temperature the pressure increases from the lower part (left) to the higher part (right) along each line and the data at lower part of each line is higher in temperature than the one at upper part. As the hole fraction decreases, Y_h increases for each temperature, so the viscosity increases. Each line slope gives the value of α as a measure of activation energy, evident from eqs. (9) and (10). It is actually related with the activation energy coefficient, a', and the total interaction energy, $q_z\Phi$, given by eq. (10). The former is expected to change with shear-rate and shear-stress, but the latter with each polymer. The interaction potential energy between a pair of segments, Φ, is assumed to be not much varying function in terms of temperature and pressure so that it is taken to be an average value given in Table I.

At the constant shear-rates from Figure 4(a), the line slopes of 96.8, 66.6, 47.8, and 14.6 decrease with the corresponding shear-rates of 0, 148, 665, 2980 s^{-1}, respectively. This can be due that as the shear-rate increases, the flowability increases and α, a measure of the activation energy, decreases as seen in Figure 5(a) for all the polymers mentioned. Using eq. (10), the activation energy coefficient, a', is calculated for each polymer given in Table V and is plotted in Figure 5(b) except PC and PMMA. It decreases as the shear-rate increases for each polymer while a' values for each polymer are close each other.

As it could be seen in Figure 4(b), the lines at the constant shear-stresses are almost parallel for HDPE and the values of α for the polymers given in Table IV plotted in Figure 6(a) are nearly independent of shear-stress. The activation energy coefficient, a', is calculated for each polymer and for polyolefins it is

Table III. Values of Parameters of eq. (9) Evaluated for η_0 at Zero Shear Rate According to eq. (8) (The Values Listed in Brackets are According to eq. (11)

Polymer	$\ln\eta^*$	α	a' ($\times10^4$)	κ	$\Delta\eta$%	R^2
LDPE	3.92 (2.55)	113.16 (157.36)	0.22 (0.31)	0.08 (0.31)	0.95 (1.62)	0.99987 (0.99963)
LLDPE	4.59 (4.52)	69.44 (70.37)	0.19 (0.19)	0.04 (0.04)	0.64 (0.71)	0.99993 (0.99991)
HDPE	6.22 (5.98)	96.82 (107.90)	0.16 (0.18)	0.01 (0.01)	0.83 (0.92)	0.99987 (0.99985)
PMMA	1.33 (1.23)	526.6 (467.9)	0.78 (0.70)	1.49 (1.65)	1.91 (1.60)	0.99941 (0.99958)
PC	−2.91 (−3.22)	672.73 (699.87)	7.16 (7.44)	92 (125.7)	3.60 (3.73)	0.99819 (0.99804)
PP	3.82 (1.85)	201.43 (312.76)	0.19 (0.29)	0.09 (0.61)	2.27 (3.94)	0.99929 (0.99768)
PS	2.17 (0.94)	346.95 (339.22)	0.22 (0.22)	0.51 (1.73)	2.53 (3.08)	0.99885 (0.99835)

Table IV. Values of Parameters of eq. (15) Evaluated for η_σ at Different Shear Stresses

Polymer	σ_c (kPa)	$\ln\eta^*$	α	a' ($\times 10^4$)	κ	$\Delta\eta$%	R^2
LDPE	36	2.43	110.16	0.22	0.35	1.56	0.99954
	60	1.64	119.63	0.23	0.76	1.30	0.99971
	99	1.15	113.61	0.22	1.24	2.12	0.99936
LLDPE	36	3.83	71.77	0.19	0.08	0.78	0.99902
	60	3.53	74.49	0.20	0.11	0.82	0.99990
	99	3.15	77.15	0.21	0.17	1.08	0.99984
HDPE	60	4.66	127.24	0.21	0.04	0.53	0.99996
	99	4.46	120.27	0.20	0.05	0.50	0.99996
	163	3.88	127.21	0.21	0.09	0.56	0.99996
PMMA	163	−4.55	716.81	1.07	532.3	1.47	0.99966
	243	−9.40	934.18	1.39	68334.5	3.89	0.99817
PC	89	−4.11	713.32	7.59	304.69	5.42	0.99591
PP	36	1.28	253.50	0.24	1.08	1.40	0.99969
	60	0.45	263.44	0.25	2.49	1.77	0.99942
	99	−1.13	288.91	0.27	11.9	3.85	0.99788
PS	89	−5.12	485.49	0.31	745.8	4.89	0.99728

plotted in Figure 6(b). Obviously, it stays almost constant for these depicted polymers. Figure 6 is drawn with the exception of PMMA, PC and PS. PMMA has larger values of α and a' comparing with the others while there is only limited levels of shear-stress available for PS and PC. From Figure 4, we can conclude that the logarithm of viscosities decreases as the constant shear-stress increases, as well as the constant shear-rate.

For all the polymers, the best fit parameters obtained from eqs. (9) and (15) are given in Tables III–V with the correlation coefficient and the mean percentage error in viscosities from eq. (20). As given in Table III, the mean percentage errors in zero

Table V. Values of Parameters of eq. (15) Evaluated for $\eta_{\dot\gamma}$ at Different Shear Rates

Polymer	$\dot\gamma_c(s^{-1})$	$\ln\eta^*$	α	a' ($\times 10^4$)	κ	$\Delta\eta$%	R^2
LDPE	148	3.86	58.2	0.11	0.08	4.19	0.99990
	665	3.46	45.1	0.09	0.12	4.74	0.99987
	2980	2.77	37.6	0.07	0.24	4.64	0.99980
LLDPE	148	4.35	49.8	0.13	0.05	3.76	0.99994
	665	4.10	38.2	0.10	0.06	3.67	0.99993
	2980	3.58	26.4	0.07	0.11	2.10	0.99997
HDPE	148	5.37	66.6	0.11	0.02	2.18	0.99998
	665	4.93	47.8	0.08	0.03	2.19	0.99998
	2980	4.50	14.6	0.02	0.05	5.83	0.99975
PMMA	148	3.35	225.6	0.34	0.20	4.66	0.99993
	665	3.06	174.1	0.26	0.27	2.43	0.99997
	2980	2.30	143.0	0.21	0.57	2.23	0.99996
PC	148	−2.02	570.0	6.07	37.71	14.84	0.99891
	665	−1.88	540.0	5.74	32.96	15.08	0.99874
	2980	−1.20	437.9	4.66	16.60	13.40	0.99880
PP	148	3.59	114.1	0.11	0.11	4.49	0.99991
	665	3.22	83.8	0.08	0.16	4.09	0.99989
	2980	2.47	64.8	0.06	0.33	5.12	0.99974
PS	148	2.64	159.6	0.10	0.32	3.59	0.99995
	665	2.18	131.9	0.08	0.50	4.34	0.99988
	2980	1.25	121.2	0.08	1.28	4.23	0.99982

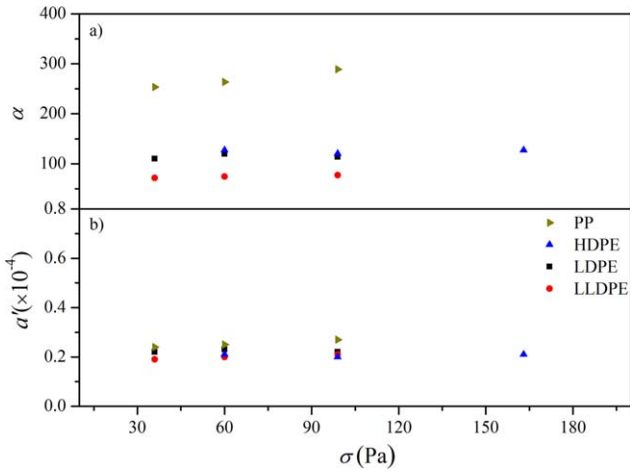

Figure 6. The shear-stress dependency of computed parameters α and a' for the polyolefins in Table I calculated by eqs. (10) and (15). [Color figure can be viewed in the online issue, which is available at wileyonlinelibrary.com.]

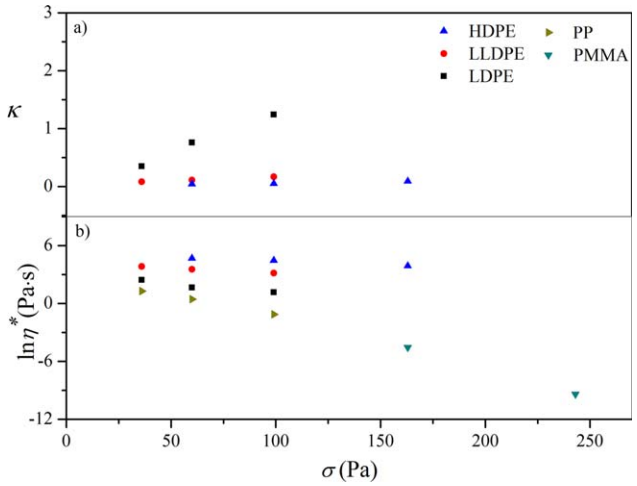

Figure 8. The shear-stress dependency of computed κ and $\ln\eta^*$ for the polymers in Table I calculated by eqs. (10) and (15). [Color figure can be viewed in the online issue, which is available at wileyonlinelibrary.com.]

shear viscosity computed by eqs. (8) and (11) range from 0.64 to 3.60 and 0.71 to 3.94, respectively. Similarly, the mean percentage errors in constant shear-stress and constant shear-rate viscosities are also calculated between 0.50 and 5.42 given in Table IV and 2.10 and 15.08 given in Table V, respectively.

Besides, the transmission coefficient, κ, in eq. (10) is also calculated and plotted in Figures 7(a) and 8(a) with respect to the shear-rate and the shear-stress, respectively. It has been found that the transmission coefficient, κ, increases linearly with the increasing shear-rate and shear-stress, yielding the molecules to jump into the holes much easily. On the other hand, the tendency of the molecules to the flowability decreases the intercepts, $\ln\eta^*$, at the viscosity axis, that represents the extrapolated viscosity values when the system dominates sufficiently large hole fraction expectedly at high temperature and low pressure in eq. (15). In other words, the thermo-occupancy function, Y_h, goes to zero. This contrary behavior of κ to $\ln\eta^*$ is obvious from Tables IV and V. Graphical results of this observation are depicted in Figures 7 and 8. Increasing the constant shear-stress given in Table IV, and the constant shear-rate given in Table V, the intercepts for HDPE decrease steadily as 4.66, 4.46, 3.88 Pa s and 5.37, 4.93, 4.50 Pa s, respectively. The decrements for the shear-rate and the shear-stress are also observed for the other polymers shown in Figures 7(b) (except for PC because of the negative values of $\ln\eta^*$) and 8b (except for PC and PS having only one computed value for $\ln\eta^*$), respectively. The calculated values of $\ln\eta^*$ of the constant shear-stress order of the materials are as follows: HDPE > LLDPE > LDPE > PP > PC > PS > PMMA. This can be interpreted such that the polymers, PC, PS, and PMMA, are bulky and smaller in size with larger pendant groups so they take the smaller values of $\ln\eta^*$. However, the lengthier structure of HDPE, LLDPE, and LDPE has the larger $\ln\eta^*$ since they are crawling with the length of their arms.

As seen from Tables III–V, PMMA, PC, PP, and PS require more activation energy than LDPE, LLDPE, and HDPE. This

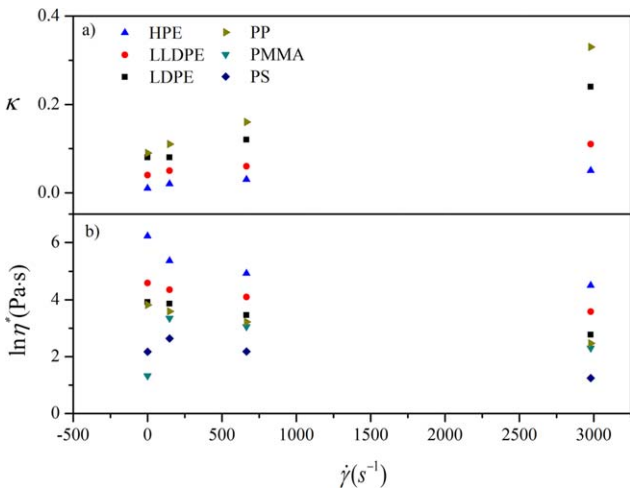

Figure 7. The shear-rate dependency of computed κ and $\ln\eta^*$ for the polymers in Table I calculated by eqs. (10) and (15). [Color figure can be viewed in the online issue, which is available at wileyonlinelibrary.com.]

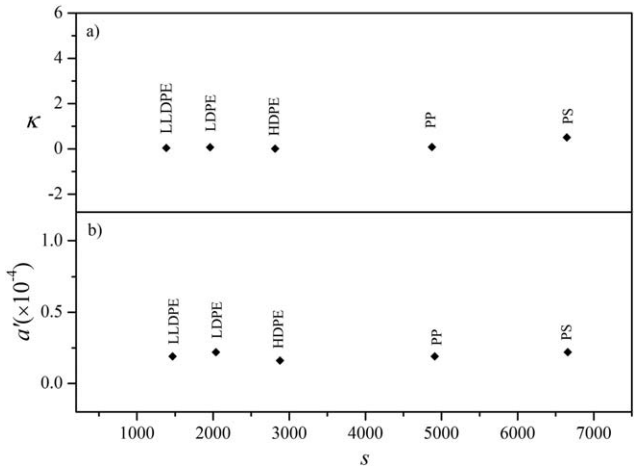

Figure 9. The chain length dependency of computed parameters κ and a' for the polymers in Table I calculated by eqs. (9) and (10).

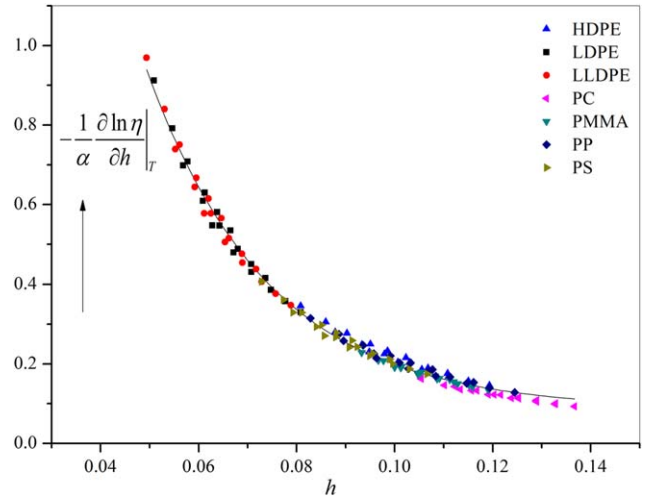

Figure 10. The derivative of logarithm of zero shear, constant shear-rate and constant shear-stress viscosities with respect to hole fraction at constant T for all polymers. Solid line represents the best fit curve through the data. [Color figure can be viewed in the online issue, which is available at wileyonlinelibrary.com.]

can be attributed to bulky allyl, methyl, and phenyl groups on the former structures.

κ and a' are plotted with respect to segmental length of the polymers in Figure 9. They are almost constant for polyolefins and PS.

At the zero shear-rate, the constant shear-rate and the constant shear-stress, the viscoholibilities given by eqs. (12–14) describe how the viscosity changes with the hole fraction as a measure of free volume at a constant temperature. The viscoholibilities at the given conditions above, divided by the structural related parameter, $-\alpha$, are plotted versus hole fraction for all polymers given in Figure 10. The parameter, $-\alpha^{-1}$, just shifts the viscoholibility in the vertical axis to overlap all the data. As the hole fraction increases on the horizontal axis, the change in logarithmic viscosity with respect to hole fraction decreases, as well. At low hole fractions, the derivative decreases rapidly with an increase of the hole fraction since a small rise in hole fraction causes a significant drop in viscosity. On the other hand, the viscoholibility does not change significantly when the hole fraction is above 0.11. This indicates the role of the pressure and temperature-dependent hole fraction in viscosity mechanism.

CONCLUSIONS

In this article, we have developed a model for the non-Newtonian viscous behavior of polymers using the Eyring Transport Theory in terms of shearing strain rate. This relation can potentially delineate a useful tool for fitting pressure and temperature dependent viscosity data. The characteristic thermodynamical parameters, P^*, V^*, T^* and the hole fraction are obtained by fitting the *PVT* data to the Simha-Somcynsky EOS. Equations (9) and (15) indicates that pressure and temperature dependent hole fraction effect on zero shear, constant shear-stress and constant shear-rate viscosities can be estimated from the evaluation of temperature affected viscosity and *PVT* characteristics. Using these formulations, any viscosity data can be predicted using the hole fraction. The logarithmic viscosity in a broad temperature and pressure range has been achieved with a reconcilable error.

NOMENCLATURE

a'	Proportionality constant of activation energy
a_i, a_i'	Numerical parameters in eqs. (17) and (18)
b_i, c_1	Numerical parameters in eq. (18)
$3c$	Total external degrees of freedom
E_a	Activation energy (J)
σ	Shear stress (N/m^2)
σ_c	Constant shear-stress (N/m^2)
h_p	Planck constant (6.626×10^{-34} J .s)
h	Hole fraction
h_i	Numerical parameters in eq. (19)
k	Boltzmann's constant (1.38×10^{-23} J/K)
k'	Jumping rate of a segment
k_i	Jumping rate of i^{th} segment
m_0	Segmental molar mass of molecules (kg)
N_A	Avogadro's number
$\tilde{P}$, $\tilde{V}$, $\tilde{T}$	Reduced pressure, volume, temperature
P^*, V^*, T^*	Characteristic pressure, volume, temperature
Q	Hole fraction and reduced volume dependent quantity in eq. (2)
q	Nonlinearity parameter in the power of shear-rate
q_z	Number of interchain nearest neighbor pairs in a lattice of coordination number
R	Gas constant (8.314 J/mol K)
r^*	Segmental location of the potential minimum
s	Number of segments of molecules
s_i	Number of segments of ith molecules
$\dot{\gamma}$	Shear-rate (s^{-1})
$\dot{\gamma}_c$	Constant shear-rate (s^{-1})
$\dot{\gamma}_0$	Zero shear-rate (s^{-1})
T	Temperature (°C or K)
v	Molar segmental volume
v^*	Characteristic molar volume of a segment
y	Occupied site fraction
Y_h	"Thermo-occupancy function," in eqs. (9) and (15)
z	Coordination number

GREEK LETTERS

α	Slope of eqs. (9) and (15)
ξ_i	Displacement volume of ith segment
$\Delta\eta$	Average percentage error in viscosity
ε	Attraction energy of a segment (k.K)
ε^*	Attractive interaction parameter of a segment of the potential minimum
η^*	Intercept of eqs. (9) and (15)
η_0, $\eta_{\dot{\gamma}}$, η_σ	Zero shear viscosity, constant shear-rate viscosity and constant shear-stress viscosity (Pa s)
λ	The distance between two successive equilibrium positions
θ_i	The angle between the shear-stress and the displacement vector of ith contiguity of a segment
κ	Transmission coefficient

λ	Distance between two successive equilibrium positions (m)
λ_1	A relative displacement of adjacent layers
$\lambda_2\lambda_3$	Surface area occupied by a segment
Φ	Mean interaction potential energy between a pair of segments (k.K)
τ	Critical shear-stress parameter

REFERENCES

1. Hieber, C. A.; Chiang, H. H. *Polym. Eng. Sci.* **1992**, *32*, 931.
2. Kadijk, S. E.; Vandenbrule, B. H. A. A. *Polym. Eng. Sci.* **1994**, *34*, 1535.
3. Sedlacek, T.; Cermak, R.; Hausnerova, B.; Zatloukal, M.; Boldizar, A.; Saha, P. *Int. Polym. Process.* **2005**, *20*, 286.
4. Yasuda, K.; Armstrong, R.C.; Cohen, R.E. *Rheol. Acta* **1981**, *20*, 163.
5. Yahsi, U. *J. Polym. Sci. Part B: Polym. Phys.* **1999**, *37*, 879.
6. Yahsi, U.; Sahin, F. *Rheol. Acta* **2004**, *43*, 159.
7. Glasstone, S.; Laidler, K. J.; Eyring, H. The Theory of Rate Processes; the Kinetics of Chemical Reactions, Viscosity, Diffusion and Electrochemical Phenomena; McGraw-Hill Book Company, Inc.: New York/London, **1941**.
8. Ree, T. S.; Eyring, H.; Ree, T. *Proc. Natl. Acad. Sci. USA* **1964**, *51*, 344.
9. Doolittle, A.K. *J. Appl. Phys.* **1951**, *22*, 1471.
10. Doolittle, A.K.; Doolittle, D.B. *J. Appl. Phys.* **1957**, *28*, 901.
11. Utracki, L. A. *Polym. Eng. Sci.* **1983**, *23*, 446.
12. Utracki, L. A. *Polym. Eng. Sci.* **1985**, *25*, 655.
13. Utracki, L. A. *Can. J. Chem. Eng.* **1983**, *61*, 753.
14. Yahsi, U. *Polym. Eng. Sci.* **1998**, *38*, 464.
15. Sahin, F.; Tav, C.; Yahsi, U. *Int. J. Thermophys.* **2006**, *27*, 1501.
16. Akdeniz; G., Yahsi; U.; Tav C. *J. Appl. Polym. Sci.* **2010**, *117*, 110.
17. Sorrentino; A., Pantani; R. *Rheol. Acta* **2009**, *48*, 467.
18. Simha, R.; Somcynsky, T. *Macromolecules* **1969**, *2*, 342.
19. Utracki, L. A.; Sedlacek, T. *Rheol. Acta* **2007**, *46*, 479.
20. Yahsi, U.; Ulutas, K.; Tav, C.; Deger, D. *J Polym Sci Part B: Polym Phys* **2008**, *46*, 2249.
21. Ree, T. S.; Ree, T.; Eyring, H. *J Phys Chem* **1964**, *68*, 3262.
22. Li, M.-F.; Ren, J.-R.; Zhu, T. Series Expansion in Fractional Calculus and Fractional Differential Equations. arXiv:0910.4819v2 [math-ph] **2009**.
23. Dalir, M.; Bashour M. *Appl. Math. Sci.* **2010**, *4*, 1021.
24. Sedlacek, T.; Zatloukal, M.; Filip, P.; Boldizar, A.; Saha P. *Polym. Eng. Sci.* **2004**, *44*, 1328.
25. Sachdev, V. K.; Yahsi, U.; Jain, R. K. *J. Polym. Sci. Part B: Polym. Phys.* **1998**, *36*, 841.